Research article

HPLC-based cytotoxicity profiling and LC-ESIQTOF-MS/MS analysis of *Helichrysum leucocephalum*

Saber Samimi-Dehkordi [a,b,c], Zahra Tayarani-Najaran [d,e], Seyed Ahmad Emami [f], Karel Nesměrák [g], Martin Štícha [h], Narjes Azizi [i], Maryam Akaberi [a,*]

[a] *Department of Pharmacognosy, School of Pharmacy, Mashhad University of Medical Sciences, Mashhad, Iran*
[b] *Student Research Committee, Mashhad University of Medical Sciences, Mashhad, Iran*
[c] *Department of Pharmacology and Toxicology, School of Pharmacy, Mashhad University of Medical Sciences, Mashhad, Iran*
[d] *Medical Toxicology Research Center, Pharmaceutical Technology Institute, Mashhad University of Medical Sciences, Mashhad, Iran*
[e] *Targeted Drug Delivery Research Center, Pharmaceutical Technology Institute, Mashhad University of Medical Sciences, Mashhad, Iran*
[f] *Department of Traditional Pharmacy, School of Pharmacy, Mashhad University of Medical Sciences, Mashhad, Iran*
[g] *Department of Analytical Chemistry, Faculty of Science, Charles University, Czech Republic*
[h] *Mass Spectrometry Laboratory, Section of Chemistry, Faculty of Science, Charles University, Prague, Czech Republic*
[i] *Forest and Rangeland Research Department, Khorasan Razavi Agricultural and Natural Resources Research and Education Center. AREEO, Mashhad, Iran*

ARTICLE INFO

ABSTRACT

Introduction: Helichrysum leucocephalum Boiss. (Asteraceae) is an endemic plant to Iran. No reports have studied the cytotoxicity of the plant. The current study aimed to evaluate the cytotoxicity of *H. leucocephalum* collected from Fars province (Iran) against MCF-7 and HDF cell lines using HPLC-based activity profiling and to annotate the active constituents by LC-ESIQTOF-MS/MS.

Methods: H. leucocephalum was collected from three locations in Fars province. The dried flowers and leaves were separately extracted by percolation using methanol. The crude extracts were fractionated by liquid-liquid partitioning with dichloromethane (DCM) and aqueous methanol. The cytotoxicity of the fractions was evaluated against MCF-7 and HDF cells by Alamarblue assay. HPLC-based activity profiling was used to track the active constituents. LC-MS dereplication strategy was used for the annotation of the compounds in the active time window. LC-MS data were preprocessed by MZmine 3.3.0 and submitted to multivariate analysis to compare the differences and similarities in the metabolites of the samples.

Results: The DCM fractions showed a dose-dependent cytotoxicity against the cancerous cells (IC50s, 9.8–105.1 µg/ml). In general, the metabolites of the flowers and their cytotoxicity were higher than the leaves. LCESIMS/MS analyses revealed that prenylated and geranylated α,β-unsaturated spiroketal phloroglucinols were among the active constituents.

Conclusion: It can be concluded that *H. leucocephalum* is a rich source of phloroglucinol derivatives with cytotoxic activities. Further phytochemical analysis is needed to characterize the bioactive components.

---

* Corresponding author.
  E-mail address: Akaberim@mums.ac.ir (M. Akaberi).

Table 1

The plant samples obtained from different locations of Fars province (Iran).

Plant sample	Region	Plant part	Herbarium No.
HLA	Ashraf	Leave	Hsbu20122328
HLAF	Ashraf	Flower	Hsbu20122328
HLN	Neyriz	Leave	Hsbu2012231
HLNF	Neyriz	Flower	Hsbu2012231
HLE	Estahban	Leave	Hsbu2012231

Table 2

The DCM and MeOH fractions obtained from different plant samples.

Crude extracts	Weight (g)	DCM fractions	Weight (g)	MeOH fractions	Weight (g)
HLA	7.8	HLAD	2.6	HLAM	4.5
HLAF	9.1	HLAFD	3.6	HLAFM	5.3
HLN	7.6	HLND	3.3	HLNM	4.1
HLNF	11.0	HLNFD	4.7	HLNFM	5.8
HLE	7.4	HLED	3.2	HLEM	3.9

1. Introduction

Helichrysum L., belonging to the Asteraceae family, consists of about 600 species worldwide, abundantly in Eurasia, Africa, and Australia [1,2]. *Helichrysum* species are herbaceous, perennials, or shrubs with dense, rectangular lanceolate, and simple to entire leaves and white or colored bracts [3]. Some species of the genus, such as *H. italicum*, are well-known as medicinal plants. Many *Helichrysum* species have been used traditionally to treat ailments, particularly infections, and as a wound healing agent in traditional and folk medicine worldwide [4]. Different compounds, including flavonoids, chalcones, α-pyrone derivatives, phloroglucinols, terpenoids, essential oils, and phenolic acids, have been reported from species of the *Helichrysum* genus [2,5].

According to the flora of Iran, 19 *Helichrysum* species, including eight endemic ones, have been reported from Iran [6]. *Helichrysum leucocephalum* Boiss. Is one of the endemic species of the genus in Iran, distributed in Yazd and Fars provinces [7]. To the best of our knowledge, only two studies have investigated the pharmacological activities of the plant. Both studies have reported the antimicrobial activities for this species. In one study, the essential oil of the leaves of *H. leucocephalum* showed antimicrobial effects against *Staphylococcus aureus* and *Escherichia coli* with a MIC (Minimum Inhibitory Concentration) value of 16 µg/ml [8]. In another study, a hydroalcoholic extract of *H. leucocephalum* was evaluated against *Streptococcus mutans* growth with MIC and MBC (Minimum Bactericidal Concentration) values of 5.6 ± 6.25, 21.6 ± 6.25 mg/ml, respectively [9]. From a phytochemical point of view, no reports have investigated the chemical constituents of the extracts from *H. leucocephalum*. However, in a study, the major volatile components were carvacrol (20.36%), acetophenone (11.17%), and azulene (7.09%) [8]. According to the literature review, there are no scientific reports investigating the cytotoxicity and safety of this valuable medicinal plant. Thus, in the present study, we aimed to evaluate the cytotoxicity of *H. leucocephalum*, track the active components with the aid of HPLC activity profiling, and identify the active constituents by liquid chromatography–electrospray ionization-quadrupole time of flight-tandem mass spectrometry (LC-ESI-QTOF-MS/MS) technique.

2. Materials and methods

2.1. Plant materials

Helichrysum leucocephalum was collected at the flowering stage in June 2020 from three different locations, Neyriz, Ashraf, and Estahban in Fars province (Iran), where are its habitats. Dr. Narjes Azizi (botanist) identified the samples. A voucher specimen for each sample was deposited at the Herbarium of Shahid Beheshti University, Tehran, Iran. After harvesting, the leaves and flowers were dried separately at room temperature in the shade and stored in paper bags until extraction (Table 1). Table 1 shows the assigned code and the herbarium number for each sample.

2.2. General experimental procedure

For extraction and preparative separation, technical grade solvents were purchased from Dr. Mojallali Company (Iran) and used after distillation. Extracts and microfractions were monitored by silica gel 60 F254-coated aluminum TLC plates (Merck, Germany), and the spots were visualized by heating the plates sprayed with vanillin sulfuric acid reagent. HPLC-grade methanol and acetonitrile and analytical-grade trifluoroacetic acid (TFA) and dimethyl sulfoxide (DMSO) were obtained from Merck Millipore (Germany). Deionized water was prepared using a TKA water deionizer (Germany).

2.3. Extraction and fractionation

After the plant materials (500 g) were powdered with an electric mill, they were extracted separately by percolation with methanol (5L, 48h). The extracts were filtered and dried under reduced pressure to afford solid residues. In the next stage, the methanol (MeOH) extracts were suspended in water and partitioned with dichloromethane (DCM). The fractions were dried under reduced pressure by a rotary apparatus to afford DCM and aqueous MeOH residues for HLA, HLAF, HLN, HLNF, and HLE (Table 2). The extracts and fractions were stored in sealed glass vials at −20 °C.

2.4. Cultivation of cancerous and non-cancerous cells

The MCF-7 and HDF cell lines were purchased from Pasture Institute, Tehran, Iran. Cancerous MCF-7 and normal HDF cells were cultured in optimal conditions (RPMI 1640 + 10% FBS; antibiotic-free) and kept at 37 °C in a CO_2 incubator. When at least 70% of the cells in the culture flask reached the confluent state, the cells were tested for cytotoxicity tests.

2.5. Cell treatment and alamar blue assay

The cytotoxicity of the fractions and HPLC microfractions were carried out according to the procedures described elsewhere [10]. For this purpose, serial drug dilutions covering a range from 100 to 2.5 µg/ml were prepared. The IC_{50} values were calculated by linear regression. The cancerous (MCF-7) and normal (HDF) cells were seeded in 96-well plates with a density of 5×10^4 cells/well and incubated at 5% CO_2 at a temperature of 37 °C for 24 h. A stock solution (50 mg/ml) of the DCM and aq. MeOH samples were prepared in DMSO and diluted (100, 50, 20, 10, 5, and 2.5 µg/ml) with the culture medium to ensure that the concentration of DMSO was less than 1% in all samples. Then, the cells were treated with different concentrations of the fractions: 100, 50, 20, 10, 5, and 2.5 µg/ml. The untreated cells served as a negative control, whereas doxorubicin-treated cells were considered as positive controls (doxorubicin with a purity of >95%; 20, 10, 5, and 2.5 mg/ml) [10]. Assays were run singly and repeated at least two times. The selectivity index was calculated as IC_{50} for HDF cells/IC_{50} for MCF-7 cells.

2.6. Microfractionation for activity profiling

HPLC-based activity profiling of the HLNFD sample was performed according to a previously established protocol [11] with some modifications. The extract (50 mg/ml in DMSO) was submitted to HPLC-PDA in ten portions of 10 mg (200 µL). The mobile phase was H_2O (A) and MeOH (B), both containing 0.05% TFA, and the following gradient profile was used: 40% B isocratic (0−2 min), 40% → 55% B (2−10 min), 55% → 75% B (10−15 min), 75% → 90% B (15−50 min), and 90% → 100% B (50−55 min), 100% B (55−75 min). The flow rate was 2 ml/min, and 5 min microfractions (between min 5 and 65) were collected into test tubes. Corresponding microfractions from the ten separations were combined. After drying, microfractions were tested for cytotoxic activity. The microfractionation was performed using a semi-preparative HPLC instrument. Isolation was performed at 22 °C on a Knauer HPLC instrument (Germany), equipped with a vacuum degasser, Smartline pump 1000, Smartline photodiode-array (PDA) detector 2800 with a UV light source, and a manual injector with a 2 ml sample loop. A Eurospher II 100-5 C_{18} column (250 mm × 8 mm, 5 µm) (Knauer, Germany) was used for reversed-phase separations. The chromatograms were obtained at 285 nm. Data processing was done by EZChrome Elite software (Germany).

2.7. LC-ESIMS instrument analysis conditions

A liquid chromatograph UHPLC Nexera XR (Shimadzu, Japan) connected with a Compact QTOF Bruker mass spectrometer (Bruker, Germany) was used. The gradient elution with binary mobile phase of methanol and 0.05% TFA was used. The Purospher® STAR RP-18 encapped (250 × 4.6 mm i.d., particle size 5 µm), tempered at 25 °C, was used with the following gradient: 40% B isocratic (0−1 min), 40% → 55% B (1−10 min), 55% → 75% B (10−15 min), 75% → 90% B (15−50 min), and 90% → 100% B (50−55 min), 100% B (55−75 min). The flow rate was 0.4 cm^3min^{-1}. The volume of the injected samples was 3 mm^3.

ESI-MS detection was performed on a Brucker QqTOF (Quadrupole-quadrupole-Time Of Flight) compact instrument operated using Compass otofControl 4.0 (Brucker Daltonics, Germany) software. Compass DataAnalysis 4.4 (Build 200.55.2969) (Brucker Daltonics, Germany) software was used for data processing. The mass spectrometer worked in the scan range of $m/z = 50–1000$. The ionization of the analytes was performed in both positive and negative ionization modes at a capillary voltage of 2.8 kV. The pressure of the nitrogen (nebulizing gas) was set to 0.50 bar. Nitrogen (3.0 dm^3min^{-1}) also served as drying gas at 220 °C. Sodium acetate served as a standard for calibration of the mass spectrometer.

2.8. MZmine data preprocessing

Raw MS data were converted into MzXML files using MassConvert software. Then, MzXML files were processed using Mzmine 3.3.0 [12]. Mass detection was carried out with a centroid mass detector. The noise level was set for both MS^1 and MS^2 levels. The ADAP chromatogram builder parameters including minimum group size of scans, minimum group intensity threshold, minimum highest intensity, and m/z (mass to charge ratio) tolerance were set. The wavelet algorithm was used for the chromatogram deconvolution and its settings including S/N (Signal to Noise ratio) threshold, intensity window SN, minimum feature height, coefficient area threshold,

Table 3

Cytotoxicity of *H. leucocephalum* DCM and MeOH fractions (IC_{50} (μg/ml)).

	HLAD	HLAFD	HLNFD	HLND	HLED	Positive Control[a]
HDF	15.90	11.24	17.19	23.58	62.75	1.31
MCF-7	105.1	45.89	9.77	41.46	55.56	3.66
SI[b]	15.1	24.5	175.9	56.9	112.9	–
	HLAM	**HLAFM**	**HLNFM**	**HLNM**	**HLEM**	
HDF	100<	100<	100<	100<	100<	1.31
MCF-7	100<	100<	100<	100<	100<	3.66

[a] Doxorubicin.

[b] Selectivity index (SI): IC_{50} in HDF cells divided by IC_{50} in the cancerous MCF-7 cells.
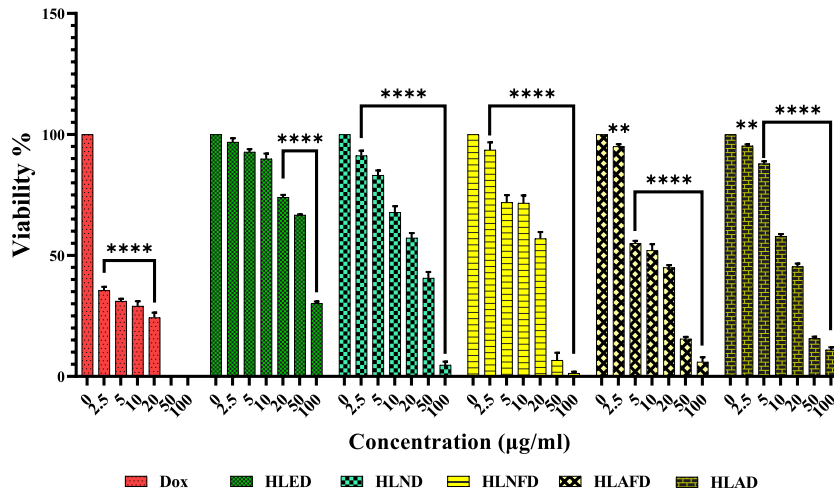
Fig. 1. Viability of HDF cells treated with different concentrations of DCM fractions after 48 h ($p < 0.05*p < 0.01**p < 0.001***$). HLED, HLND, and HLAD refer to the DCM fraction from leave of plant samples collected from Estahban, Neyriz, and Ashraf regions in Fars province. HLNFD and HLAFD refer to the DCM fraction of flower samples collected from Neyriz and Ashraf regions in Fars province (Iran).
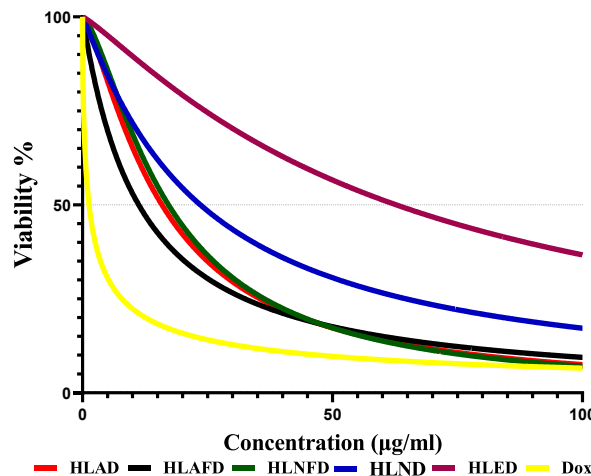

Fig. 2. IC_{50} values of the DCM samples against HDF cells after 48 h. HLED, HLND, and HLAD refer to the DCM fraction of leave samples collected from Estahban, Neyriz, and Ashraf regions in Fars province, respectively. HLNFD and HLAFD refer to the DCM fraction of flower samples collected from Neyriz and Ashraf regions in Fars province (Iran), respectively.

peak duration range, and RT (Retention Time) wavelet range were optimized. Chromatograms were deisotoped using the isotopic peaks grouper algorithm with an optimized m/z tolerance, RT tolerance, maximum charge of 2 and the representative isotope used was the most intense.
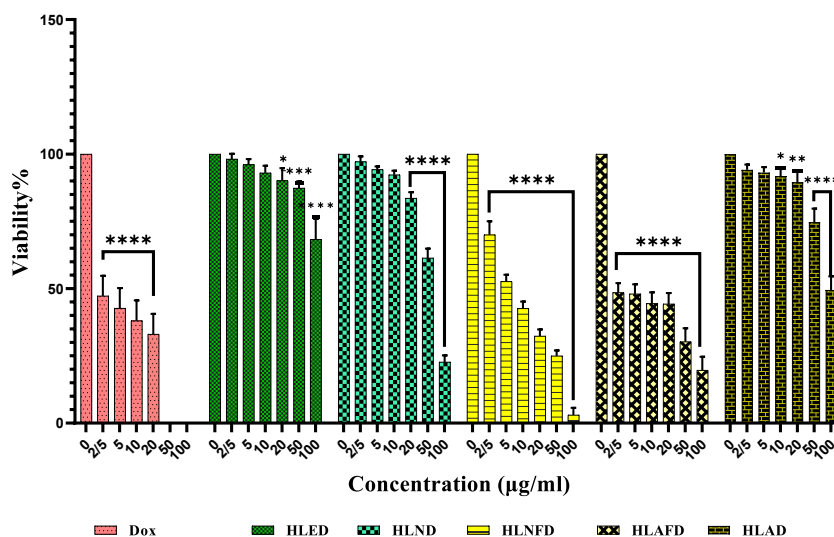
Fig. 3. Viability of MCF-7 cells treated with different concentrations of DCM fractions after 48 h (p < 0.05*p < 0.01**p < 0.001***). HLED, HLND, and HLAD refer to the DCM fraction of leave samples collected from Estahban, Neyriz, and Ashraf regions in Fars province. HLNFD and HLAFD refer to the DCM fraction of flower samples collected from Neyriz and Ashraf regions in Fars province (Iran).
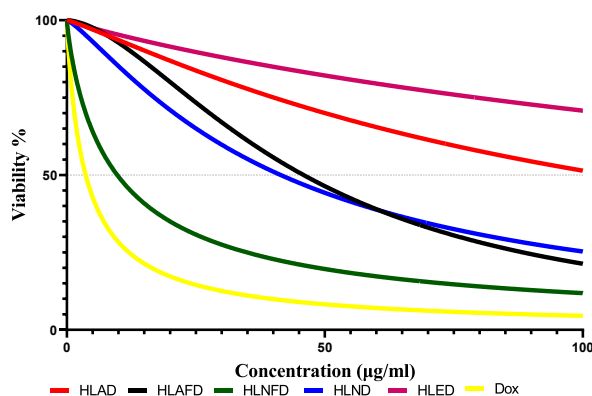
Fig. 4. IC$_{50}$ values of the DCM fractions against MCF-7 cells after 48 h. HLED, HLND, and HLAD refer to the leave of plant samples collected from Estahban, Neyriz, and Ashraf regions in Fars province, respectively. HLNFD and HLAFD refer to the flowers of plant samples collected from Neyriz, and Ashraf regions in Fars province (Iran), respectively.

2.9. Multivariate analysis

The normalized matrix extracted from MZmine was imported to SIMCA 14.0 (Umetrics, Sweden). The matrix was pretreated with Pareto variance scaling and a PCA (Principal Component Analysis) model was generated with the data matrix. Heat maps were created using the FreeClust platform [13,14]. Hierarchical clustering analysis was performed based on Euclidean distance.

3. Results & discussion

3.1. Cytotoxic activity

In this study, the cytotoxic effects of the DCM and aq. MeOH fractions obtained from the flower and leaves of *H. leucocephalum* collected from three regions, Neyriz, Estahban, and Ashraf of Fars province (Iran) were evaluated against HDF and MCF-7 cells. No cytotoxicity was observed for the aq. MeOH fractions. All DCM fractions showed a dose-dependent cytotoxic activity (2.5, 5, 10, 20, 50, and 100 µg/ml) to some extent against the cancerous and normal cells (Table 3, Figs. 1–4). The plant samples from Neyriz, including the leaves (HLND) and flowers (HLNFD), showed the highest cytotoxic effects against MCF-7 cells compared to samples from Ashraf and Estahban regions (Table 3). Among all samples, HLNFD exhibited the highest selectivity index. Thus, sample HLNFD was submitted for further phytochemical analysis to track active components. In addition, the lowest cytotoxic activity against MCF-7 cells was observed for the leave samples from Ashraf (HLAD). However, the flower sample from this region showed a high cytotoxicity compared
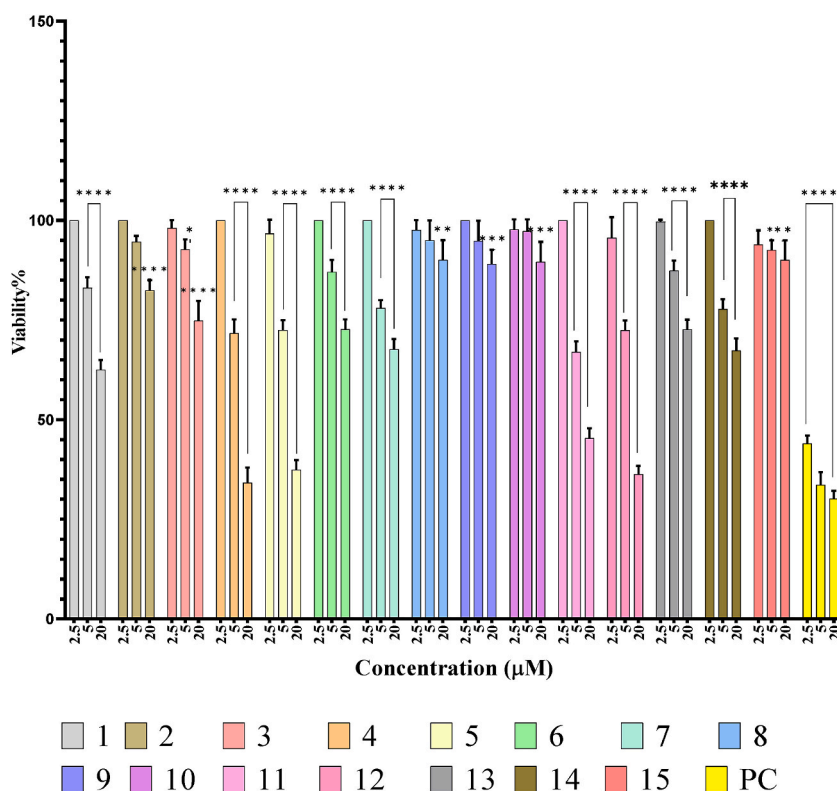
Fig. 5. Viability of MCF-7 cells treated with concentrations 2.5, 5, 20, and 100 μg/ml of HPLC microfractions (1–15) after 48 h (p < 0.05*p < 0.01**p < 0.001***).

to the other samples. Moreover, it can be concluded that the flowers may contain more cytotoxic compounds than the leaves.

HLED, HLND, and HLAD refer to the DCM fraction of leave samples collected from Estahban, Neyriz, and Ashraf regions in Fars province, respectively. HLNFD and HLAFD refer to the DCM extract of flower samples collected from Neyriz, and Ashraf regions in Fars province (Iran), respectively. HLEM, HLNM, and HLAM refer to the MeOH fraction of leave samples collected from Estahban, Neyriz, and Ashraf regions in Fars province, respectively. HLNFM and HLAFM refer to the MeOH fraction of flower samples collected from Neyriz and Ashraf regions in Fars province (Iran), respectively.

According to the best of our knowledge, there is no previous report investigating the cytotoxicity of *H. leucocephalum*. Therefore, the current study evaluated the cytotoxic activity of *H. leucocephalum* for the first time. However, based on a literature survey, other *Helichrysum* species showed cytotoxicity. For example, Sagbo et al. have evaluated the anti-proliferative and genotoxic activities of the MeOH extract from *Helichrysum petiolare* Hilliard & B.L. Burtt against mouse melanoma cells (B16F10) and human melanoma cells (MeWo) at concentrations 12.5–200 μg/ml [15]. The extract showed cytotoxicity against both cancerous cell lines in a dose-dependent manner. Further analysis showed that the extract could increase apoptosis in both cell lines by inducing cell cycle arrest at the S phase and the early M phase in B16F10 and MeWo cells, respectively. Moreover, at the tested concentrations, the extract exhibited genotoxic effects [15]. In a study reported by Lourens et al. [16], chloroform: MeOH (1:1) extract of *H. aureum* displayed cytotoxic effects against transformed human kidney epithelial (Graham) cells, breast adenocarcinoma (MCF-7), and glioblastoma (SF-268) cells at concentration 0.1 mg/ml with inhibition of 5%, 7%, and 35%, respectively [17].

Interestingly, studies show that the non-polar fractions like DCM and EtOAc might be more cytotoxic than polar fractions like MeOH. For instance, Matic et al. have studied the cytotoxic activities of different fractions of *H. zivojinii* Cernjavski & Soska, including *n*-hexane, DCM, EtOAc, *n*-butanol (BuOH), and MeOH fractions against human cervix adenocarcinoma HeLa, human melanoma Fem-x, human myelogenous leukemia K562, and human breast adeno-carcinoma MDA-MB-361 cells. All fractions exerted dose-dependent cytotoxic activities on the cancerous cells to some extent. However, *n*-hexane and DCM fractions exhibited the highest cytotoxic effects compared to cisplatin as a positive control. EtOAc and BuOH fractions displayed less cytotoxicity than *n*-hexane and DCM fractions, and the MeOH fraction showed the lowest activity [18]. Likewise, ethanol:EtOAc (1:9, 5:5, 9:1, and 0:100) extracts from *H. plicatum* showed cytotoxic activity against PC3, HeLa and K562 human cancer cell lines *in vitro*. All tested extracts exhibited moderate activity against HeLa cells (41.9–42.1 μg/ml) whereas the extract obtained with 100% EtOAc was the most active against K562 and PC3 cell lines with IC$_{50}$s 25.9 and 39.2 μg/ml, respectively [19]. In addition, there are several investigations reporting the cytotoxic activities of the essential oil from different *Helichrysum* species. For instance, the volatile oil of *H. odoratissimum* (L) Sweet. Exhibited moderate cytotoxicity against brine shrimp larvae with LC$_{50}$ of 31.16 μg/ml [20]. Afoulous et al. reported that the essential oil of *H. gymnocephalum* was active against MCF-7 tumor cell lines with IC$_{50}$ = 16 ± 2 mg/L [21].
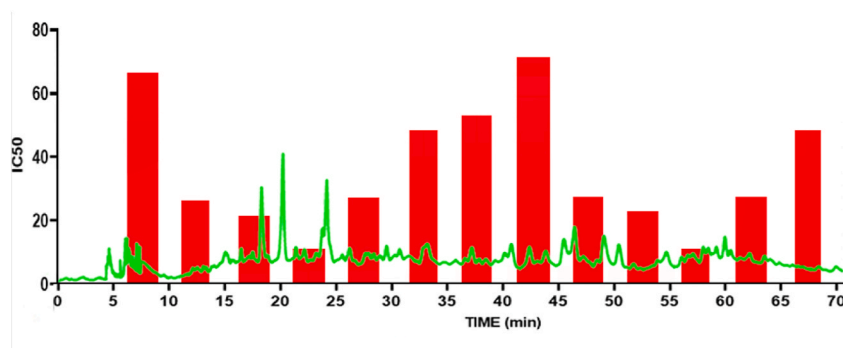
Fig. 6. HPLC-based activity profiling of the dichloromethane extract of *H. leucocephalum* (HLNFD). The PDA chromatogram (285 nm) of a separation of 10 mg of extract on a semipreparative reverse phase HPLC column is shown. Activity of 5 min microfractions is indicated with colored columns for cytotoxic activity, expressed as IC_{50}.
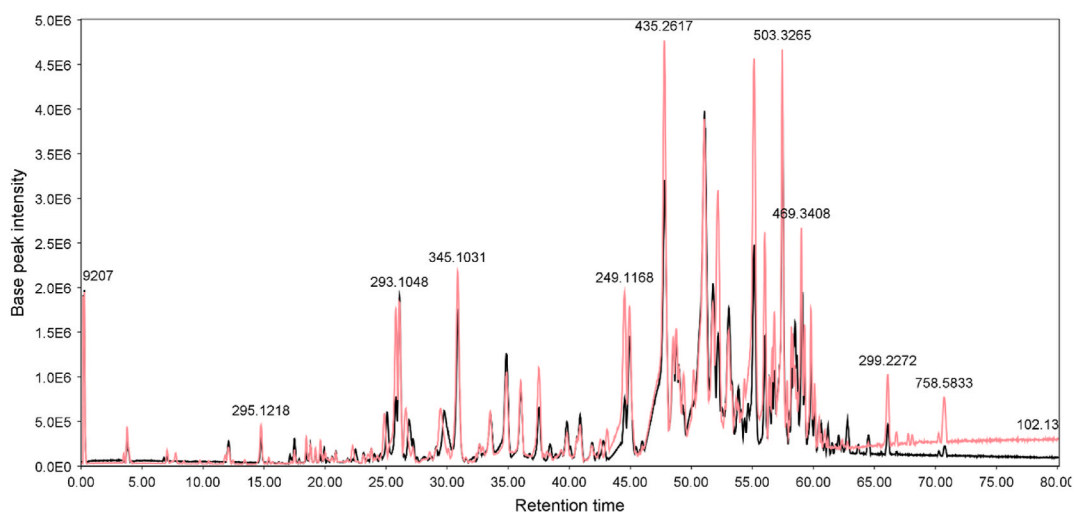

Fig. 7. LC-MS chromatograms of the flower DCM fractions of *H. leucocephalum* collected from Neyriz (black) and Ashraf (pink) in positive ionization mode. ESIMS: base peak chromatogram (BPC); *m/z* 50–1000; column Purospher® STAR RP-18 encapped (250 × 4.6 mm, 5 μm; Merck). MeOH 0.05% TFA/aq. 0.05 TFA in 80 min, a flow rate of 0.7 ml/min. The following gradient mode was employed: 0.0−1.0 min: 40% B isocratic, 1.0−10.0 min: 40−55% B, 10.0−15.0 min: 55−75% B, 15.0−50.0 min: 75−90% B, 50−55 min: 90.0−100.0% B, and 55.0−75.0 min: 100% B. (For interpretation of the references to color in this figure legend, the reader is referred to the Web version of this article.)

3.2. Microfractionation for activity profiling

The cytotoxic constituents in the DCM extract of *H. leucocephalum* (HLNFD) were tracked by HPLC-based activity profiling [11,22, 23]. The activity of the microfractions were measured by Alamarblue assay against MCF-7 cells (Fig. 5). An activity profile of 13 5 min fractions and the corresponding LC−PDA traces are shown in Fig. 6. The highest activities were observed for the time window between 10-25 and 45–60 min (Fig. 6).

3.3. LC-ESIQTOF-MS/MS analysis

The DCM fractions from the *H. leucocephalum* samples were analyzed separately by LC-ESIQTOF-MS and LC-ESIQTOF-MS/MS (Figs. 7 and 8).

3.3.1. Annotation of compounds
The compounds of interest were annotated by comparing their molecular mass and fragmentation patterns with those of available libraries and databases including Dictionary of Natural Products and an in-house library. Based on the results of the biological test, microfractions 4 (20–25 min) and 11 (55–60 min) contained the most cytotoxic compounds in the UV chromatogram (Fig. 6). Because the microfractionation and MS analysis were performed on two separate instruments, the peaks of interests in the MS chromatogram were localized in time windows 25–30 min and 55–60 min. However, wider active windows were included in order to involve the
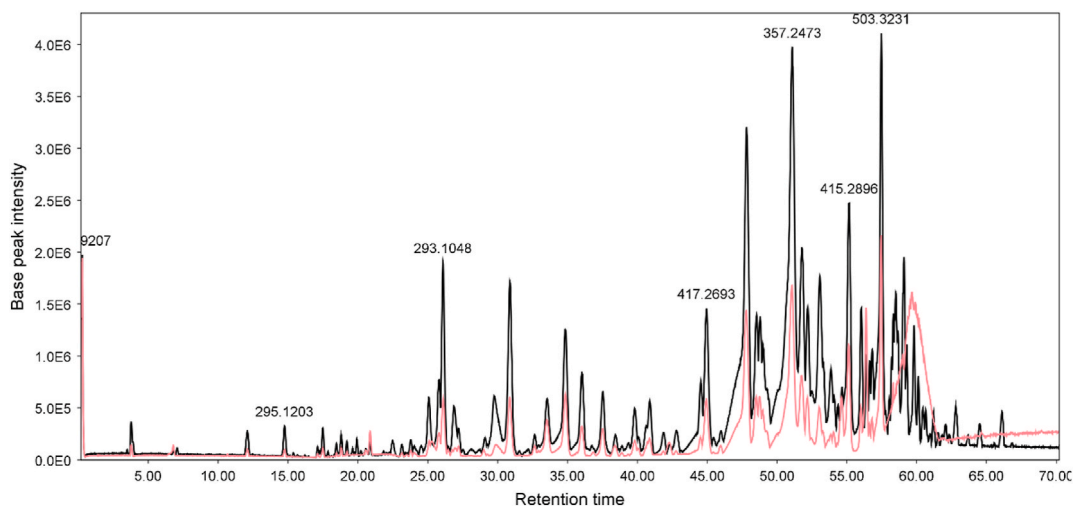
Fig. 8. LC-MS chromatograms of the leave (pink) and flower (black) DCM fractions of *H. leucocephalum* collected from Neyriz in positive ionization mode. ESIMS: base peak chromatogram (BPC); *m/z* 50–1000; column Purospher® STAR RP-18 encapped (250 × 4.6 mm, 5 µm; Merck). MeOH 0.05% TFA/aq. 0.05 TFA in 80 min, a flow rate of 0.7 ml/min. The following gradient mode was employed: 0.0−1.0 min: 40% B isocratic, 1.0−10.0 min: 40−55% B, 10.0−15.0 min: 55−75% B, 15.0−50.0 min: 75−90% B, 50−55 min: 90.0−100.0% B, and 55.0−75.0 min: 100% B. (For interpretation of the references to color in this figure legend, the reader is referred to the Web version of this article.)
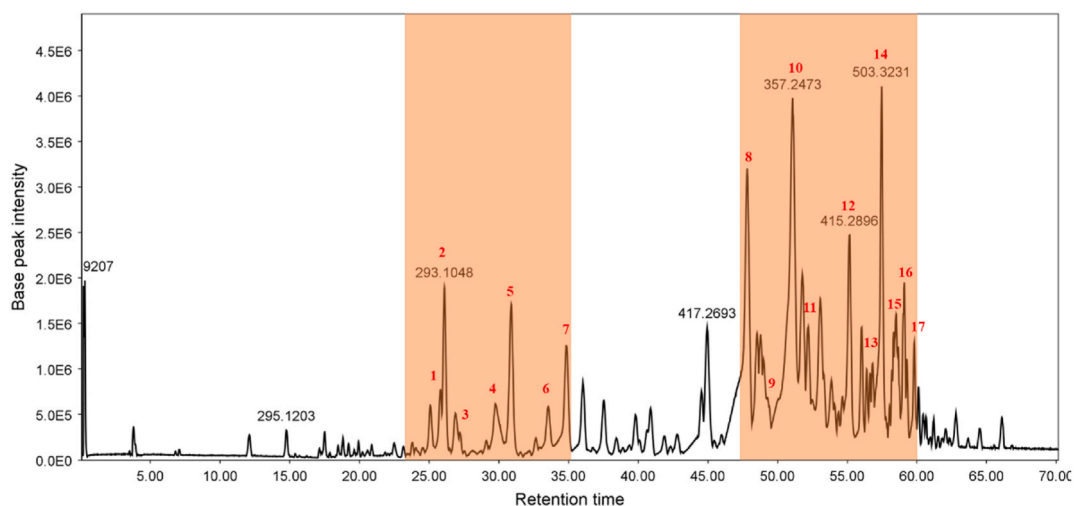

Fig. 9. The peak number of the detected compounds in the active time windows for the DCM fraction of *Helichrysum leucocephalum* flowers in positive ionization mode.
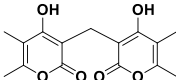
neighbor windows with moderate cytotoxicity (Fig. 9). Then, the spectral information of the peaks of interest, including their retention time and mass spectrum characteristics, was extracted (Table 4).

3.3.1.1. Homodimer pyrones. Compound **2** produces the [M+H]$^+$ ion at *m/z* 293 in the mass spectrum. Data from tandem mass spectrometry (MS^n) showed that ion 293 breaks into ion 153, 141, and 125 (Scheme 1). According to literature survey [24–26], this fragmentation pattern can be attributed to a homopyrone derivative namely helipyrone C (Fig. 10A & B). Homodimer pyrones, including helipyrone A, B, and C, have been previously isolated from other species of the *Helichrysum* genus [2,11].

3.3.1.2. Prenylated α,β-unsaturated spiroketal phloroglucinols. Compound **11** produced [M+H]$^+$ and [M − H]$^−$ ions at *m/z* 401 and 399 in the positive and negative ion modes, respectively. Data from tandem mass spectrometry (MS^n) in the negative ion mode showed that ion 399 breaks mainly into ion 287 resulted from a 112 Da loss. However, less abundant ions such as 330, 275, 262, 219, 194, and 152 were also observed (Fig. 11). By comparing the observed MS^1 and MS^2 data with our in-house library made of phloroglucinol derivatives from the genus *Helichrysum*, the molecular ion at 399 *m/z* can be attributed to an α,β-unsaturated spiroketal phloroglucinol
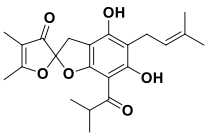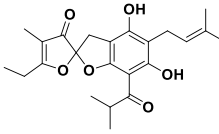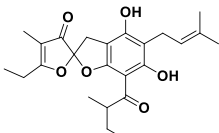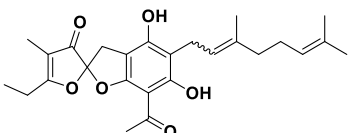
Table 4

Annotation of the compounds in the chromatograms of the flower DCM fraction of *H. leucocephalum* (peak number in Fig. 9, retention time in the chromatogram, m/z of $[M+H]^+$ and $[M - H]^-$ ion, MS^n, identity, and reference to mass spectrum used for confirmation of the substance).

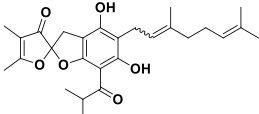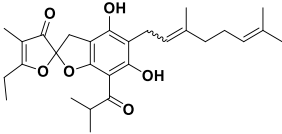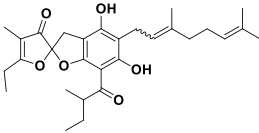| No.	r_t/min	M	MS^+	MS^-	MS/MS^+	MS/MS^-	Annotation	Ref.
1	25.55	468	467.2493	465.1672	**MS^2 [467]:** **313.1115 (100)**, 259.0640 (51.5), 221.0840 (25.4), 153.0571 (6.2), 105.0355 (62.3), 69.0719 (18.5)	**MS^2 [467]:** 325.1161 (25.0), **313.1154 (100)**, 139.0436 (50.0)	Unresolved	–
2	25.92	292	293.1048	–	**MS^2 [293]:** 153.0567 (36.9), **141.0567 (100)**, 125.0617 (6.7)	-	Helipyrone C	[11]
3	27.18	404	405.1603	–	**MS^2 [405]:** 265.1109 (50.0), **253.1108 (100)**, 247.1001 (23.7), 235.1000 (30.9), 193.0520 (46.9), 181.052 (43.7), 153.0568 (43.7), 141.0567 (37.5) **MS^3 [261]:** **205.0524 (100)**	-	Unresolved	–
4	29.48	332	333.2102	331.2010	–	–	Unresolved	–
5	30.88	372	373.1011	–	**MS^2 [373]:** **153.0571 (100)**	–	Unresolved	–
6	33.51	450	451	449	**MS^2 [451]:** **309.1177 (100)** 291.1066 (3.8) 273.1534 (7.7) 255.0699 (25.7) 231.0695 (39.4) 217.0900 (24.2) 177.0215 (7.1) 105.0354 (10.4) 69.711 (2.6)	**MS^2 [449]:** 380.1720 (18.4) 363.1689 (36.8) 337.1165 (94.7) **321.1212 (100)** 312.1060 (11.2) 307.1050 (12.1) 297.1204 (26.3) 253.0567 (34.7) 228.0476 (9.5) **MS^3 [449 → 321]:** 277.0574 (47.3) 265.0577 (26.4) **243.0722 (100)** 215.0765 (15.4) 199.0800 (30.9) 171.0832 (13.6) 145.0304 (85.4) 121.0288 (11.8)	Unresolved	–
7	34.84	450	451.2542	449.2449	**MS^2 [451]:** **327.1283 (100)**, 309.1174 (24.0), 255.0695 (29.3), 217.0894 (8), 177.0211 (3.4), 105.0359 (15.3), 69.0723 (4.6)	-	Unresolved	–
8	47.84	434	435.2589	433.2488	**MS^2 [435]:** 311.1324 (31.7), **255.0688 (100)**, 219.1047 (10), 195.0316 (10.0), 177.0206 (21.7), 105.0356 (10.8) **MS^3 [435 → 311]:** 255.0689 (14.6), 195.0316 (84.3), **177.0208 (100)**, 149.0253 (1.8),	**MS^2 [433]:** 364.1771 (8.5), 349.1536 (6.7), 336.1817 (3.8), **321.1218 (100)**, 309.1215 (12.7), 296.1131 (7.9), 279.1103 (4.4), 253.0577 (16.9), 145.0338 (1.1) **MS^3 [433 → 364]:** 349.1521 (7.0), 321.1217 (52.9),	Unresolved	–

Table 4 (*continued*)

| No.	r_t/min	M	MS$^+$	MS$^-$	MS/MS$^+$	MS/MS$^-$	Annotation	Ref.
					109.0304 (9.1), 81.0355 (2.9)	307.1056 (6.2), 292.1396 (9.7), 270.1098 (8.2), 268.9607 (11.8), 243.0735 (15.0), **174.9726 (100)**, 145.0335 (16.8)		
9	49.42	386	387.2582	385.2466	**MS^2 [387]:** 263.1324 (53.1), 219.1053 (20.0), **207.0686 (100)**, 189.0577 (18.1) **MS^3 [207]:** 161.0623 (28.1), 133.0674 (21.8), 115.0567 (45.3), **107.0513 (100)**, 91.0568 (36.0), 79.0568 (81.2)	**MS^2 [385]:** **273.1205 (100)**, 205.0565 (13.3) **MS^3 [273]:** 243.0726 (51.5), **229.0568 (100)**, 217.0931 (69.7), 162.0354 (42.4)	Tentative NEW	–
10	51.10	356	357.2477	–	**MS^2 [357]:** **153.0569 (100)**, 125.0618 (4.7) **MS^3 [153]:** **125.0617 (100)**, 111.0453 (19.2), 105.0463 (33.8), 99.0461 (44.6), 95.0509 (23.1), 83.0514 (61.5), 77.0406 (18.5)	–	Unresolved	–
11	52.17	400	401.2743	399.2631	**MS^2 [401]:** 277.1473 (80.4), 259.1365 (21.7), **221.0839 (100)**, 219.1046 (77.2), 203.0729 (64.1), 163.0411 (10.9), 69.0720 (10.4) **MS^3 [277]:** 221.0845 (14.5), 219.1054 (18.8), **203.0737 (100)**, 175.0783 (29.0), 163.0417 (18.2),	**MS^2 [399]:** 355.2727 (24.0), 330.1920 (7.1), 315.1681 (6.7), **287.1362 (100)**, 219.0723 (13.7) **MS^3 [287]:** 269.1252 (70.6), **243.0663 (100)**, 229.0500 (55.3), 217.0858 (77.6), 201.0182 (49.4)	Helispiroketal C	[11]
12	55.27	414	415.2902	413.2823	**MS^2 [415]:** 291.1656 (92.9), 273.1544 (25.0), **235.1017 (100)**, **219.1064 (100)**, 217.0906 (78.6), 163.0424 (12.9), 69.0726 (10.0) **MS^3 [415 → 291]:** **217.0905 (100)** **MS^3 [415 → 275]:** 219.1061 (36.4), **163.0423 (100)**, 135.0470 (17.6)	**MS^2 [413]:** **301.1525 (100)**, 233.0880 (14.0) **MS^3 [301]:** 283.1346 (81.4), 271.0984 (32.1), 257.0827 (74.4), 243.0664 (74.4), 229.0509 (48.8), **217.0860 (100)**, 201.0183 (44.2), 162.0277 (20.9), 125.0526 (65.1)	Tentative NEW	–
13	56.62	440	441.3061	439.2948	**MS^2 [441]:** 317.1799 (4.2), 249.1161 (95.8), **193.0525 (100)**, 137.1349 (4.0), 81.0722 (21.7) **MS^3 [441 → 249]:** 193.0523 (60.0), **175.0415 (100)**, 147.0467 (14.1)	**MS^2 [439]:** 395.3041 (5.1), 327.1679 (7.5), **301.1517 (100)**, 259.1041 (81.2), 247.1036 (12.5), 234.0956 (15.0), 191.0400 (13.7), 166.0316 (5.2)	Tentative NEW	–

Table 4 (*continued*)

No.	r_t/min	M	MS$^+$	MS$^-$	MS/MS$^+$	MS/MS$^-$	Annotation	Ref.
14	57.48	502	503.3236	501.3119	**MS^2 [503]:** 311.1328 (58.0), **255.0691 (100)**, 177.0209 (8.7), 81.0721 (12.0)	**MS^2 [501]:** **363.1685 (100)**, 321.1208 (81.7), 253.0569 (19.7) **MS^3 [363]:** 321.1205 (3.86), 285.1206 (7.3), 268.9605 (12.0), 241.1297 (2.9), 217.1293 (3.4), **174.9721 (100)**, 145.0322 (18.9)	Unresolved	–
15	58.31	454	455.3226	453.3105	**MS^2 [455]:** 331.1954 (6.4), **263.1316 (94.6)**, **207.0681 (100)**, 137.1346 (5.1), 81.0721 (25.8) **MS^3 [455 → 263]:** 207.0680 (21.3), **189.0572 (100)**, 161.0619 (18.7), 133.0668 (9.3), 107.0510 (10.7)	**MS^2 [453]:** 341.1838 (8.1), **315.1677 (100)**, 273.1199 (8.1), 261.1197 (12.3), 248.1116 (14.6), 205.0559 (13.5) **MS^3 [453 → 315]:** 297.1520 (59.1), 271.0957 (68.2), 243.0668 (59.1), **217.0844 (100)**, 139.0686 (63.6)	Helispiroketal G	[11]
16	58.31	468	469.3396	467.3168	MS2 [469]:	**MS^2 [467]:** 423.3356 (8.0), 355.1983 (9.4), **329.1834 (100)**, 287.1354 (86.6), 275.1292 (13.4), 262.1263 (15.8), 219.0714 (15.8), 194.0631 (5.8) **MS^3 [467 → 329]:** 311.1652 (51.4), **287.1290 (100)**, 285.1870 (77.1), 283.1697 (77.1), 271.0976 (42.8), 259.1332 (71.4), 243.0659 (54.3), 219.0664 (37.1), 207.0646 (80.0), 177.1268 (62.8)	Tentative NEW	–
17	59.02	482	483.3221	481.3435	**MS^2 [483]:** 359.2278 (7.0), **291.1638 (100)**, 235.1002 (73.6), 219.1051 (50.0), 81.0722 (34.5) **MS^3 [483 → 291]:** 235.1004 (17.1), **217.0895 (100)**	**MS^2 [481]:** 437.3521 (8.5), 369.2142 (10.7), **343.1916 (100)**, 301.1511 (85.4), 289.1509 (13.4), 276.1427 (21.9), 233.0874 (21.9), 208.0793 (8.6)	Tentative NEW	–

which was reported for the first time from *H. oocephalum* in our previous work [11]. Scheme 2, Figs. 11A and 11B show the plausible fragmentation pattern for **11** based on previous similar studies reporting the fragmentation pathways of phloroglucinol derivatives [24–26]. Therefore, compound **11** was identified tentatively as helispiroketal C [11].

Compound **9** and **12** showed a very similar fragmentation pattern to that of **11**. Compound **9** produced [M+H]$^+$ and [M − H]$^-$ ions at m/z 387 and 385 in the positive and negative modes, respectively. Compound **12** produced [M+H]$^+$ and [M − H]$^-$ ions at m/z 415 and 413 in the positive and negative modes, respectively. The mass of **11** differed from that of **9** and **12** by 14 amu; 14 amu more than compound **9** and 14 amu less than compound **12**. Moreover, in MS/MS$^-$, compounds **9** and **12** displayed ions at m/z 273 and 301, respectively, with a 14 amu difference from the ion at m/z 287 observed in **11**. Therefore, **9** might lack one methyl group compared to compound **11**. And compound **12** might have one more methyl group than **11**, probably located in the acyl group. Based on the observed molecular masses and fragmentation patterns, compound **9** and **12** are phloroglucinol derivatives bearing an α,β-unsaturated spiroketal (Table 4). Based on the literature review, these compounds have not been reported and their exact structure should be
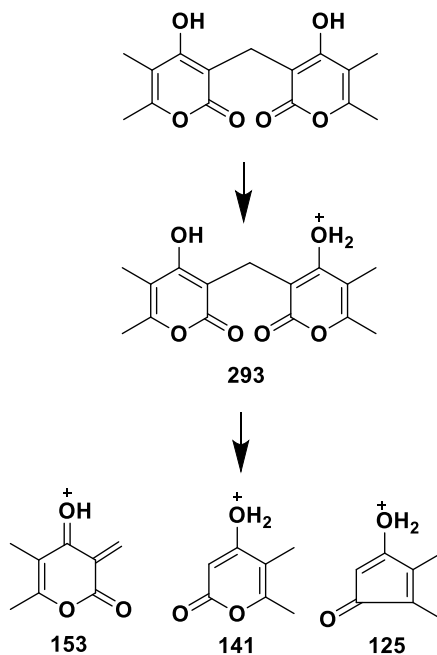
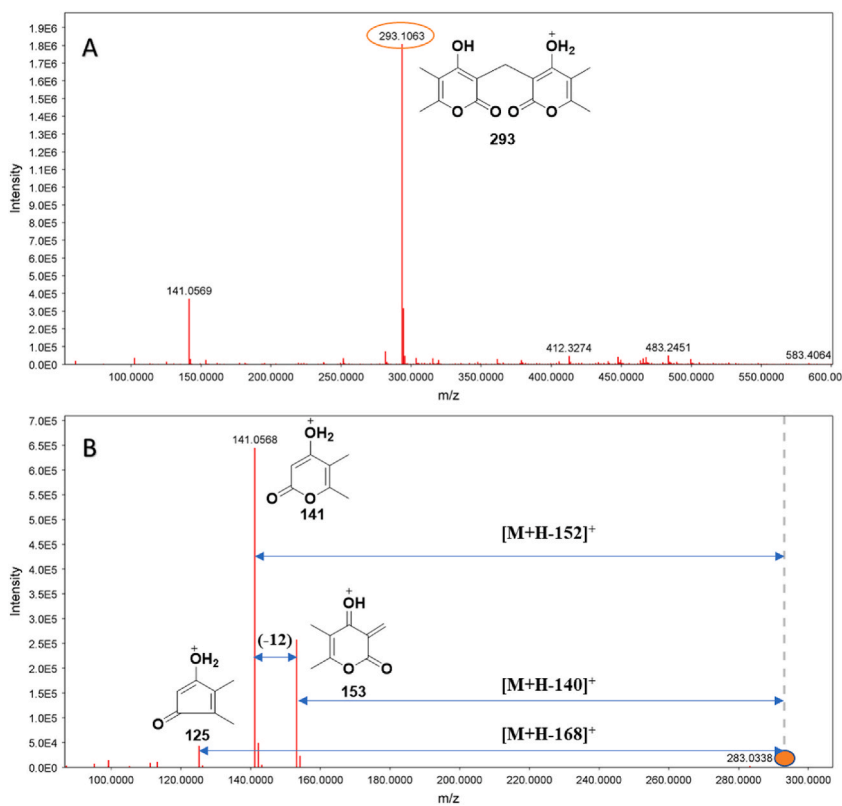**Scheme 1.** The plausible MS/MS fragmentation pattern for compound **2** in positive ionization mode.

Fig. 10. MS^1 (A) and MS^2 (B) spectra of compound **2** (helipyrone C), [M+H]$^+$ = 293.
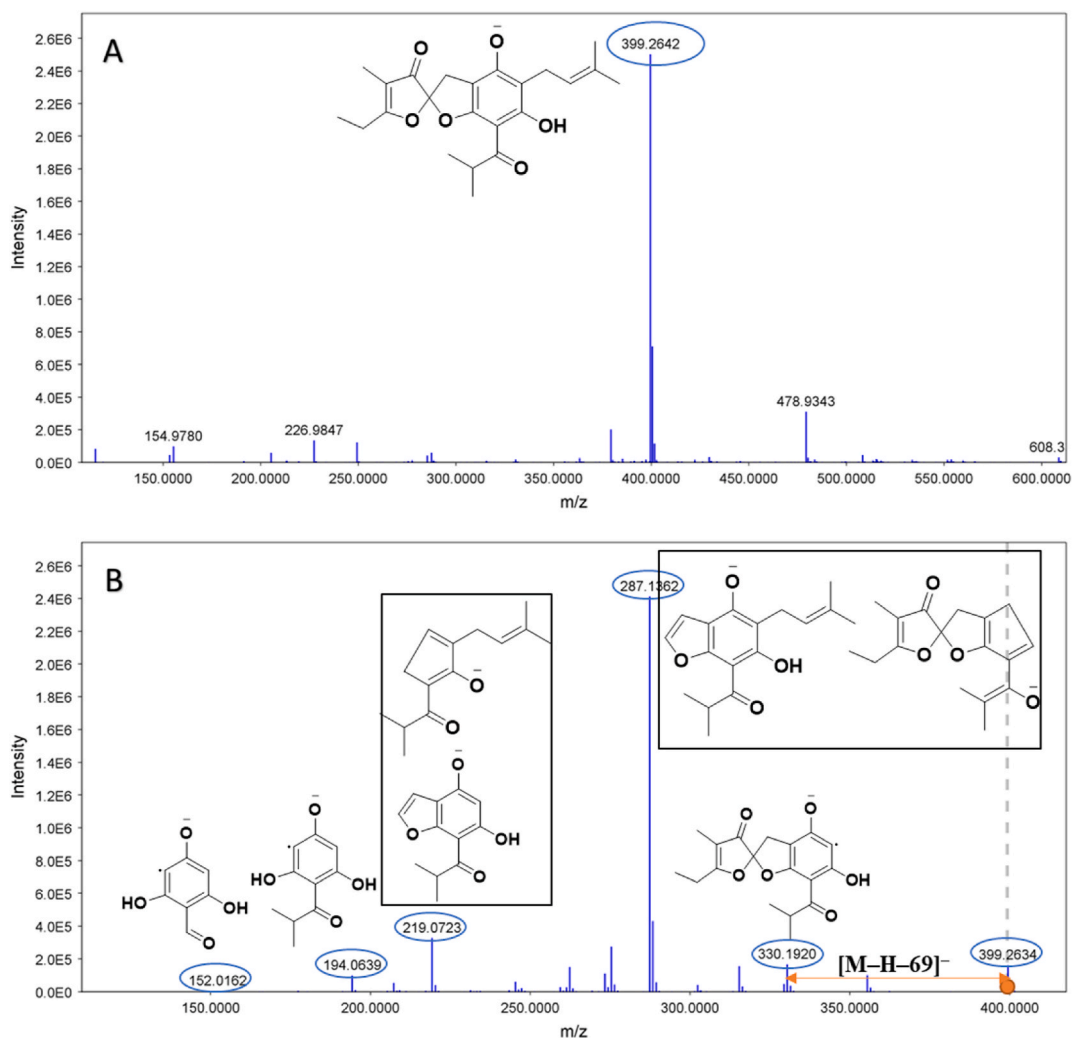
Fig. 11. MS^1 (A) and MS^2 (B) spectra of compound **11** (helispiroketal C), [M−H]$^−$ = 399.

confirmed in future studies by the NMR techniques.

3.3.1.3. Geranylated α,β-unsaturated spiroketal phloroglucinols. Compound **16** produced [M+H]$^+$ and [M − H]$^−$ ions at *m/z* 469 and 467 in the positive and negative modes, respectively. The fragmentation pattern of this compound was different from that of **9, 11**, and **12** but with some similarities. In the MS/MS$^−$ of compound **16**, ions at *m/z* 423, 398, 355, 329, 315, 302, 287, 275, 262, 245, 219, 207, and 194 were detected. Of these, ions at *m/z* 329 and 287 with intensities of 100.0 and 86.6 were the most abundant. Similarly, in the MS/MS$^−$ of compound **11**, ions at *m/z* 355, 330, 315, 302, 287, 275, 262, 245, 219, 207, and 194 were detected, of which ion at *m/z* 287 was the most intense peak. As it obvious, the observed ions from the ion at *m/z* 355 to the ion at *m/z* 194 were identical in both compounds. Interestingly, the compound **16** differed from **11** by 69 amu, which can show the existence of an extra isoprenyl moiety in **16**. In addition, in our previous study, we could isolate geranylated α,β-spiroketal phloroglucinol 15E- and 15Z-helispiroketals G and H with a molecular mass of 454 [11]. In the current study, compound **15** displayed [M+H]$^+$ and [M − H]$^−$ ions at *m/z* 455 and 453 in the positive and negative modes, respectively, with an estimated mass 454, similar to the molecular mass of helispiroketal G. Compound **15** exhibited a very similar fragmentation pattern to compound **16** with a 14 amu mass difference. Thus, according to the MS and MS/MS data and similarity search with our in-house library, compound **15** and **16** were tentatively identified as geranylated homologues of helispiroketal C (Table 4, Fig. 12, and Scheme 3) [24–26].

Compound **13** with a [M+H]$^+$ ion at *m/z* 441 in a positive mode and a [M−H]$^−$ ion at *m/z* 439 in a negative mode and compound **17** with a [M+H]$^+$ ion at *m/z* 483 in a positive mode and a [M−H] $^−$ ion at *m/z* 481 in a negative showed very similar ion fragmentation pattern with compound **15** and **16**. Compound **13** (estimated mass 440) differed 14 amu with compound **15** (estimated mass 454), indicative of the lack of a methyl moiety. The observed mass for compound **17** (482) was 28 amu more than that of compound **15**. Therefore, compounds **13** and **17** were also plausibly identified as geranylated α,β-spiroketal phloroglucinols. A proposed
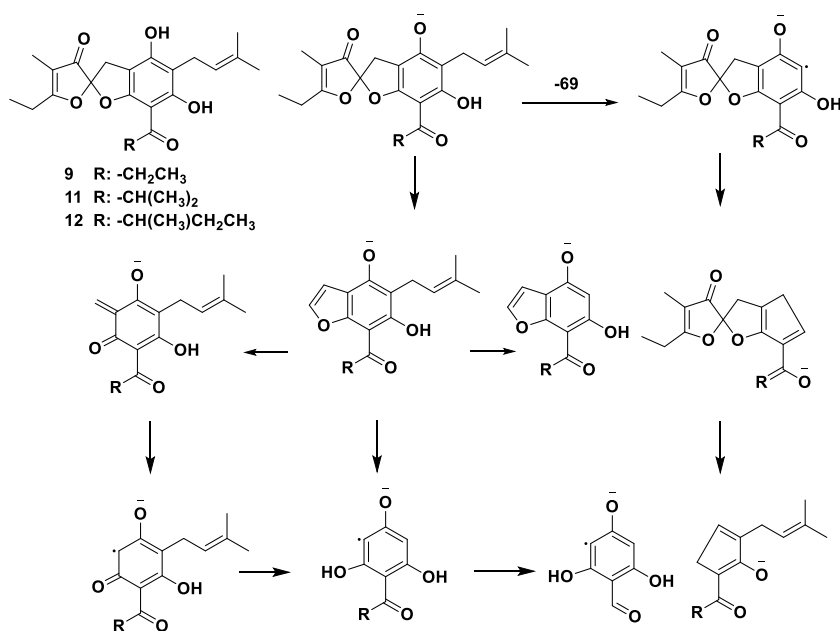
Scheme 2. The plausible MS/MS fragmentation pattern for compound **11,** a prenylated α,β-unsaturated spiroketal phloroglucinol derivative, in negative ionization mode.
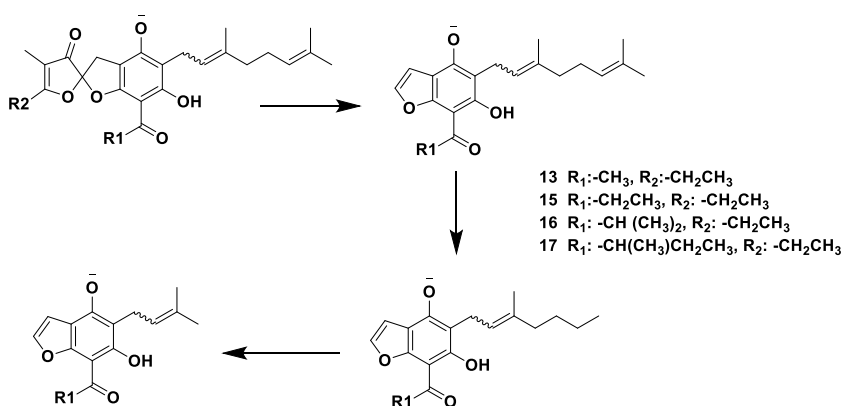

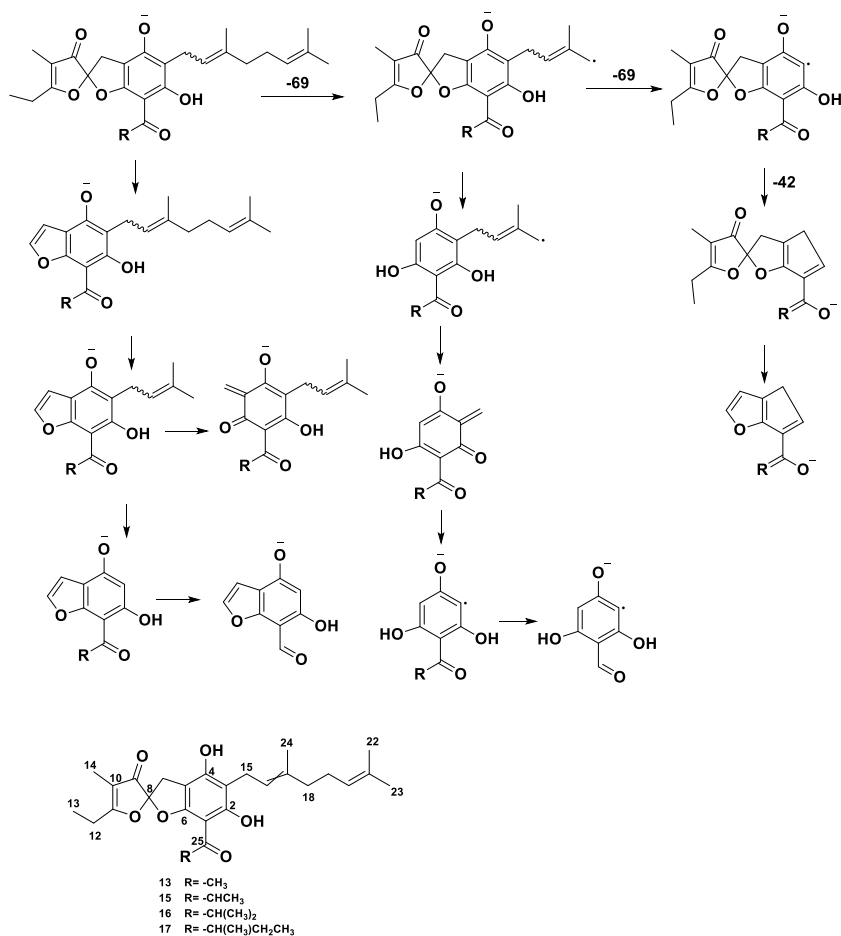**Fig. 12.** The plausible MS^n fragmentation pathway for the geranylated α,β-unsaturated spiroketal phloroglucinol derivatives.

fragmentation pattern is illustrated in Scheme 3 for these derivatives [24–26].

Fig. 13 shows the identified compounds from the active windows. According to the literature review, the difference of the geranylated α,β-unsaturated spiroketal phloroglucinol derivatives is in the substitutions of the acyl group (carbon 1) and the substitutions in carbon 9 [11]. Based on the previous similar reported compounds, the moieties at carbon 9 can be methyl or ethyl while the substitutions attached to carbon 1 can be oxoethyl, oxopropyl, 2-methyl oxopropyl, and 2-methyl oxobutyl.

3.4. Multivariate analysis

A scatter plot using a PCA model was depicted (Fig. 14). Although the variations in the samples are small and the samples from different regions showed a good correlation, the PCA score plot (P1) divided the samples into two main groups corresponding to flowers (orange) and leaves (green). The PCA gave a model that represented 99.6% of the original dataset information. The parameters of this model (R2 X = 0.593 and Q2 = 0.27) validated the quality of this PCA.

The data were visualized using a heat-map of the HCA results to view the differences across the dataset and provide an overview of all detected metabolites (Fig. 15). As obvious from the figure, the flower and leave samples were grouped in two distinct clusters. In addition, the detected metabolites in flower samples were higher than the leave samples. Interestingly, the HLED sample contained the least metabolites, resulting in the least cytotoxic activity.

Scheme 3. The plausible MS/MS fragmentation pattern for geranylated α,β-unsaturated spiroketal phloroglucinols in negative ionization mode.
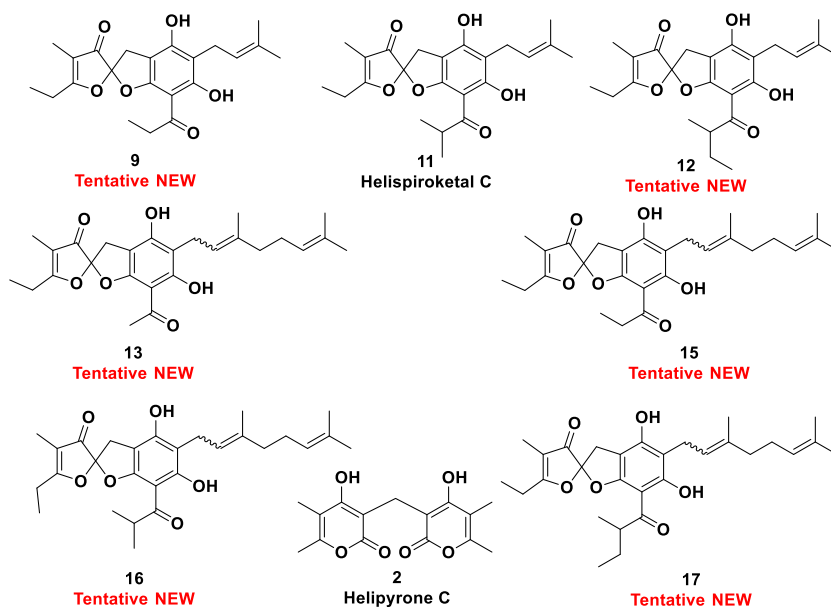

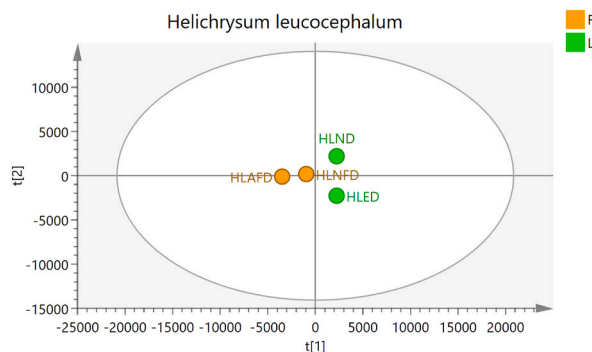Fig. 13. The compounds annotated in the active time windows.

Fig. 14. PCA score plot derived from multivariate statistical analysis of LC-ESIQTOF-MS profiling data acquired from *Helichrysum leucocephalum* samples. HLED and HLND refer to the DCM fraction of leave samples collected from Estahban and Neyriz regions in Fars province, respectively. HLNFD and HLAFD refer to the DCM extract of flower samples collected from Neyriz, and Ashraf regions in Fars province (Iran), respectively.
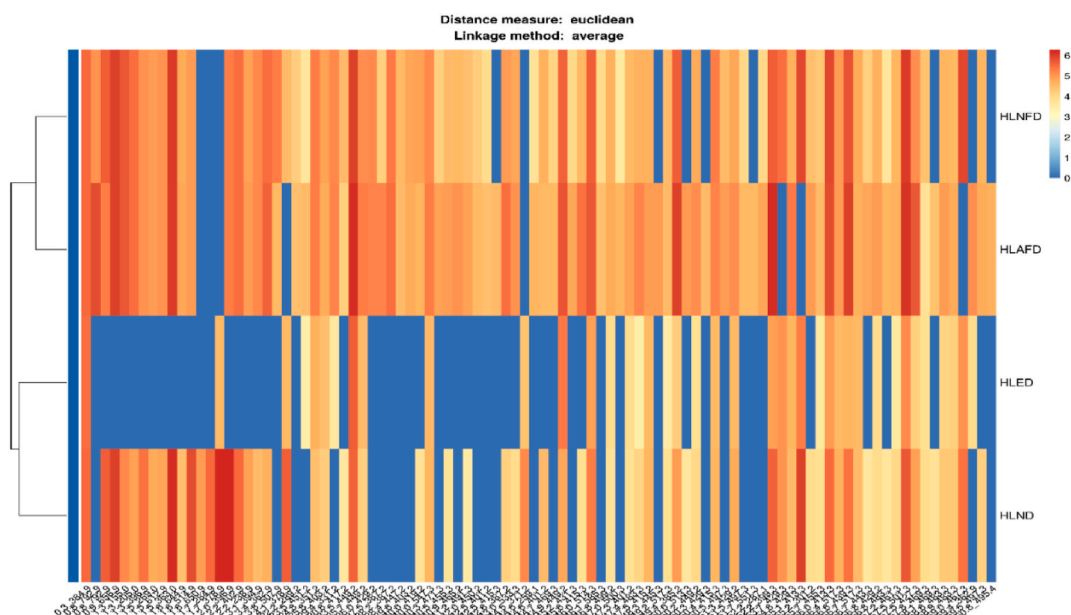

Fig. 15. Heat-map of the metabolites in the samples of *Helichrysum leucocephalum*. In this analysis, only LCESIMS/MS results in negative ionization mode were used. The colors represent the abundance of compounds in the samples; the most abundant compounds are red and the absent compounds are blue. The X-axis shows the detected ions in the time interval from 0 to 60 min. (For interpretation of the references to color in this figure legend, the reader is referred to the Web version of this article.)

4. Conclusion

In this study, *H. leucocephalum*, especially the DCM fraction of the flowers (IC_{50} for HLNFD: 9.8 μg/ml), showed a dose-dependent cytotoxicity against MCF-7 cancerous cells. The HPLC-based activity profiling and LC-MS analysis revealed that compounds belonging to homodimer pyrones and prenylated and geranylated heterodimer phloroglucinols bearing an α,β-unsaturated spiroketal group might be the active constituents. Plausible fragmentation pathways were predicted for each category of the annotated compounds. However, supplementary phytochemical studies are necessary to complete the characterization of the tentative new compounds using other spectroscopical data, including NMR, in order to confirm the proposed structures.

Funding

Data availability

All data to support the conclusions have been provided.

Ethics statement

Not applicable.

CRediT authorship contribution statement

Saber Samimi-Dehkordi: Writing – original draft, Formal analysis, Data curation. **Zahra Tayarani-Najaran:** Resources, Methodology, Data curation. **Seyed Ahmad Emami:** Writing – review & editing, Project administration, Formal analysis. **Karel Nesměrák:** Validation, Software, Investigation, Formal analysis, Data curation. **Martin Štícha:** Validation, Investigation, Data curation. **Narjes Azizi:** Resources, Investigation, Data curation. **Maryam Akaberi:** Writing – review & editing, Supervision, Project administration, Funding acquisition, Conceptualization.

Declaration of competing interest

The authors declare that they have no known competing financial interests or personal relationships that could have appeared to influence the work reported in this paper.

Acknowledgments

References

[1] I. Süntar, E.K. Akkol, H. Keles, E. Yesilada, S.D. Sarker, Exploration of the wound healing potential of *Helichrysum graveolens* (Bieb.) Sweet: isolation of apigenin as an active component, J. Ethnopharmacol. 149 (1) (2013) 103–110, https://doi.org/10.1016/j.jep.2013.06.006.

[2] M. Akaberi, A. Sahebkar, N. Azizi, S.A. Emami, Everlasting flowers: phytochemistry and pharmacology of the genus *Helichrysum*, Ind. Crops Prod. 138 (2019) 111471, https://doi.org/10.1016/j.indcrop.2019.111471.

[3] A. Ghahreman, Iranian Choromophites (Botanical Systematic), Iran University Press, Tehran, 1994.

[4] J. Mastelic, O. Politeo, I. Jerkovic, N. Radosevic, Composition and antimicrobial activity of *Helichrysum italicum* essential oil and its terpene and terpenoid fractions, Chem. Nat. Compd. 41 (1) (2005) 35–40.

[5] E. Czinner, K. Hagymasi, A. Blazovics, A. Kery, É. Szőke, E. Lemberkovics, The in vitro effect of Helichrysi flos on microsomal lipid peroxidation, J. Ethnopharmacol. 77 (1) (2001) 31–35, https://doi.org/10.1016/s0378-8741(01)00258-6.

[6] V. Mozaffarian, Compositae: Anthemideae & Echinopeae—In Flora of Iran, No 59, Research Institute of Forests and Rangelands, Tehran, 2008.

[7] POWO, Plants of the World Online, Faciltated by the Royal Botanic Gardens, Kew, 2022. Published on the internet.

[8] M.A.F. Jahromi, S. Dehshahri, S. Forouzandeh Samani, Volatile Composition, Antimicrobial and free radical scavenging activities of essential oil and total extract of *Helichrysum leucocephalum* Boiss, Trends Pharmacol. Sci. 3 (3) (2017) 193–200.

[9] M. Motamedifar, A. Nozari, E. Azhdari Ghasrodashti, *In vitro* investigation of hydro-alcoholic extract of *Helichrysum leucocephalum* on the inhibition of *Streptococcus mutans* growt, J. Dent. Biomater. 4 (4) (2017) 484–488.

[10] M. Akaberi, S.A. Emami, M. Vatani, Z. Tayarani-Najaran, Evaluation of antioxidant and anti-melanogenic activity of different extracts of aerial parts of *N. sintenisii* in murine melanoma B16F10 Cells, Iran, J. Pharm. Res. 17 (1) (2018) 225.

[11] M. Akaberi, O. Danton, Z. Tayarani-Najaran, J. Asili, M. Iranshahi, S.A. Emami, M. Hamburger, HPLC-based activity profiling for antiprotozoal compounds in the endemic Iranian medicinal plant *Helichrysum oocephalum*, J. Nat. Prod. 82 (4) (2019) 958–969, https://doi.org/10.1021/acs.jnatprod.8b01031.

[12] T. Pluskal, S. Castillo, A. Villar-Briones, M. Orešič, MZmine 2: modular framework for processing, visualizing, and analyzing mass spectrometry-based molecular profile data, BMC Bioinf. 11 (1) (2010) 1–11.

[13] A. Bozicevic, M. Dobrzyński, H. Bie, F. Gafner, E. Garo, M. Hamburger, Automated comparative metabolite profiling of large LC-ESIMS data sets in an ACD/MS workbook suite add-in, and data clustering on a new open-source web platform FreeClust, Anal. Chem. 89 (2017) 12682–12689, https://doi.org/10.1021/acs.analchem.7b02221.

[14] M. Akaberi, Z.T. Najaran, N. Azizi, S.A. Emami, Metabolite profiling and antiprotozoal activity of three endemic Iranian *Helichrysum* species, Ind. Crops Prod. 174 (2021) 114196, https://doi.org/10.1016/j.indcrop.2021.114196.

[15] I.J. Sagbo, W. Otang-Mbeng, Anti-proliferative and genotoxic activities of the *Helichrysum petiolare* Hilliard & BL Burtt, Sci. Pharm. 88 (4) (2020) 49, https://doi.org/10.3390/scipharm88040049.

[16] A. Lourens, S. Van Vuuren, A. Viljoen, H. Davids, F. Van Heerden, Antimicrobial activity and in vitro cytotoxicity of selected South African *Helichrysum* species, South Afr. J. Bot. 77 (1) (2011) 229–235, https://doi.org/10.1016/j.sajb.2010.05.006.

[17] A.O. Akinfenwa, I.J. Sagbo, M. Makhaba, W.T. Mabusela, A.A. Hussein, *Helichrysum* genus and compound activities in the management of diabetes mellitus, Plants 11 (10) (2022) 1386, https://doi.org/10.3390/plants11101386.

[18] I.Z. Matić, I. Aljancić, V. Vajs, M. Jadranin, N. Gligorijević, S. Milosavljević, Z.D. Juranić, Cancer-suppressive potential of extracts of endemic plant *Helichrysum zivojinii*: effects on cell migration, invasion and angiogenesis, Nat. Prod. Commun. 8 (9) (2013) 1291–1296.

[19] D. Bigović, K. Savikin, T. Janković, N. Menković, G. Zdunić, T. Stanojković, Z. Djurić, Antiradical and cytotoxic activity of different *Helichrysum plicatum* flower extracts, Nat. Prod. Commun. 6 (6) (2011) 819–822.

[20] O.A. Lawal, I.A. Ogunwande, A.A. Kasali, A.R. Opoku, A.O. Oyedeji, Chemical composition, antibacterial and cytotoxic activities of essential oil from the leaves of *Helichrysum odoratissimum* grown in South Africa, J. Essent. Oil-Bear. Plants 18 (1) (2015) 236–241, https://doi.org/10.1080/0972060X.2014.901618.

[21] S. Afoulous, H. Ferhout, E.G. Raoelison, A. Valentin, B. Moukarzel, F. Couderc, J. Bouajila, *Helichrysum gymnocephalum* essential oil: chemical composition and cytotoxic, antimalarial and antioxidant activities, attribution of the activity origin by correlations, Molecules 16 (10) (2011) 8273–8291, https://doi.org/10.3390/molecules16108273.

[22] O. Potterat, M. Hamburger, Combined use of extract libraries and HPLC-based activity profiling for lead discovery: potential, challenges, and practical considerations, Planta Med. 80 (14) (2014) 1171–1181, https://doi.org/10.1055/s-0034-1382900.

[23] O. Potterat, M. Hamburger, Concepts and technologies for tracking bioactive compounds in natural product extracts: generation of libraries, and hyphenation of analytical processes with bioassays, Nat. Prod. Rep. 30 (4) (2013) 546–564, https://doi.org/10.1039/c3np20094a.

[24] G. Peron, D.R. Pant, S.S. Shrestha, S. Rajbhandary, S. Dall'Acqua, An integrated LC-ESI-MS(n) and high resolution LC-ESI-QTOF approach for the identification of phloroglucinols from Nepalese *Hypericum japonicum*, Molecules 25 (24) (2020), https://doi.org/10.3390/molecules25245937.

[25] C.-J. Wang, Y.-Q. Jiang, D.-H. Liu, X.-H. Yan, S.-C. Ma, Characterization of phloroglucinol derivatives and diterpenes in *Euphorbia ebracteolata* Hayata by utilizing ultra-performance liquid chromatography/quadrupole time-of-flight mass spectrometry, J. Pharm. Anal. 3 (4) (2013) 292–297, https://doi.org/10.1016/j.jpha.2013.01.002.

[26] L. Sleno, R. Daneshfar, G.P. Eckert, W.E. Müller, D.A. Volmer, Mass spectral characterization of phloroglucinol derivatives hyperforin and adhyperforin, Rapid Commun. Mass Spectrom. 20 (18) (2006) 2641–2648, https://doi.org/10.1002/rcm.2650.